SUPPLEMENTARY ONLINE MATERIALS

for

Cryo-EM structure of the spinach chloroplast ribosome reveals the location of plastid-specific ribosomal proteins and extensions

Michael Graf[1], Stefan Arenz[1], Paul Huter[1], Alexandra Dönhöfer[1], Jiří Nováček[2], Daniel N. Wilson[1,3,*]

[1] Gene Center, Department for Biochemistry and Center for integrated Protein Science Munich (CiPSM), University of Munich, 81377 Munich, Germany

[2] Central European Institute of Technology (CEITEC), Masaryk University, Kamenice 5, 62500 Brno, Czech Republic.

[3] Department of Biochemistry and Molecular Biology, University of Hamburg, 20146 Hamburg, Germany.

* To whom correspondence should be addressed. Tel: +49 89 2180 76903; Fax: +49 89 2180 76945; Email: wilson@lmb.uni-muenchen.de.

SUPPLEMENTARY FIGURES

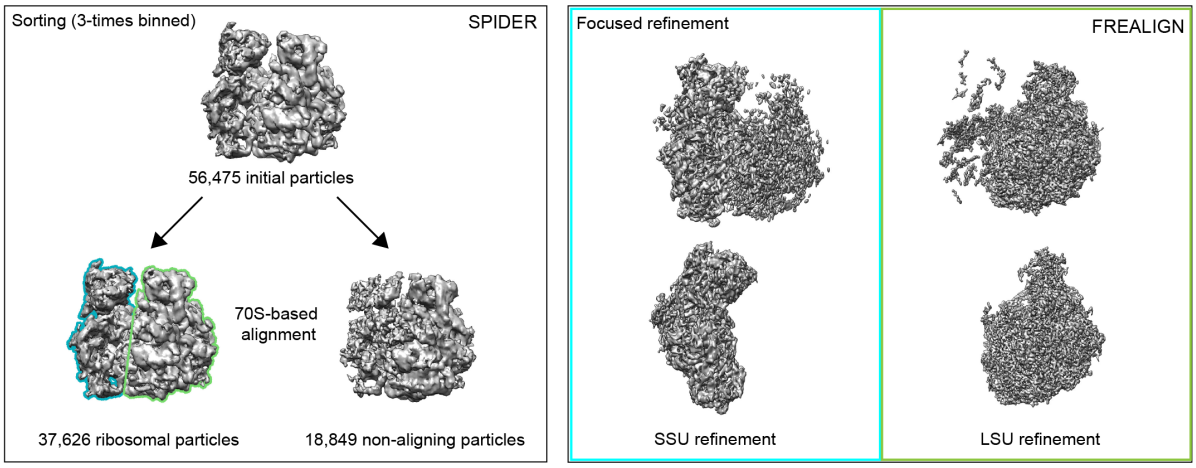

Figure S1: *In silico* sorting and refinement of the chloroplast SSU and LSU. (**A**) *In silico* sorting was performed using SPIDER (2), starting with an initial 56,475 particles that yielded after removal of non-aligning particles (18,849), a dataset of 37,626 ribosomal particles. (**B**) Subsequently, focused alignment and refinement of the SSU and LSU was performed in FREALIGN (3).

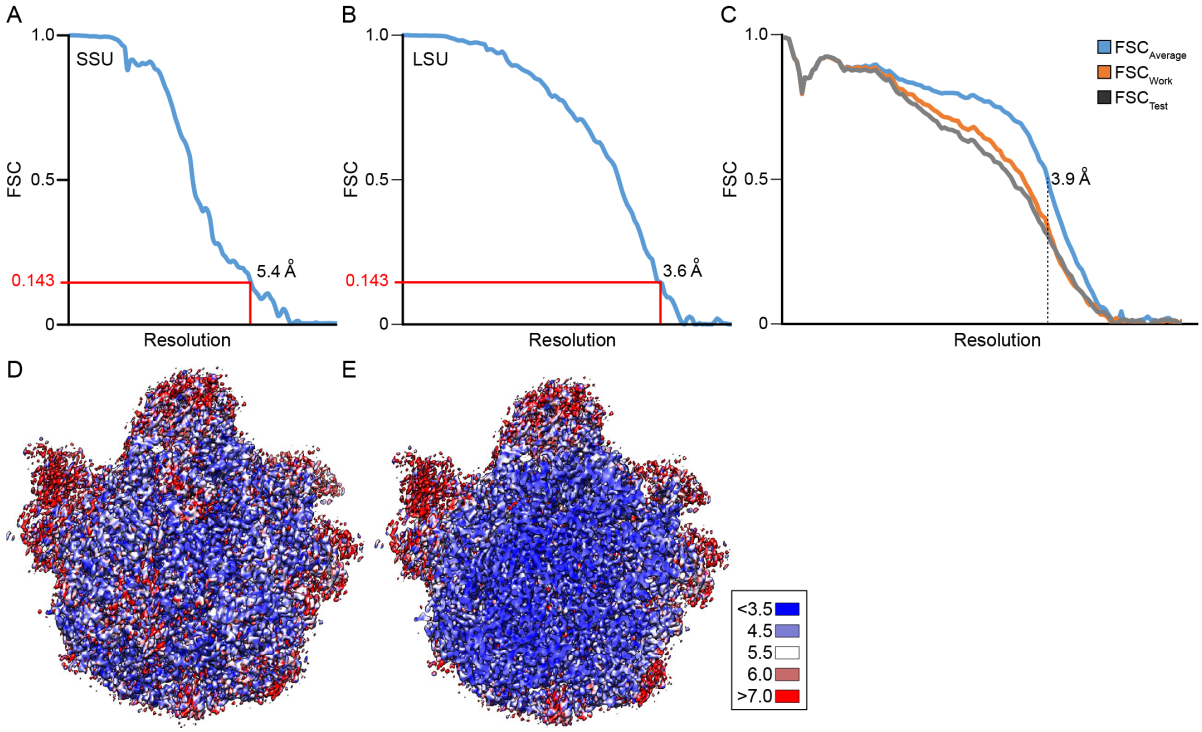

Figure S2: Resolution of the cryo-EM reconstruction of the chloroplast SSU and LSU. (**A,B**) Fourier-shell correlation curve (FSC) of the refined final map of the chloroplast (**A**) SSU and (**B**) LSU, indicating the average resolution is 5.4 Å and 3.6 Å, respectively. (**C**) Fit of models to maps. FSC curves calculated between the refined model and the final map (blue), with the self- and cross-validated correlations in orange and black, respectively. Information beyond 3.6 Å was not used during refinement and preserved for validation. (**D**) Overview and (**E**) transverse section through the chloroplast LSU colored according to the local resolution as calculated using ResMap (1).

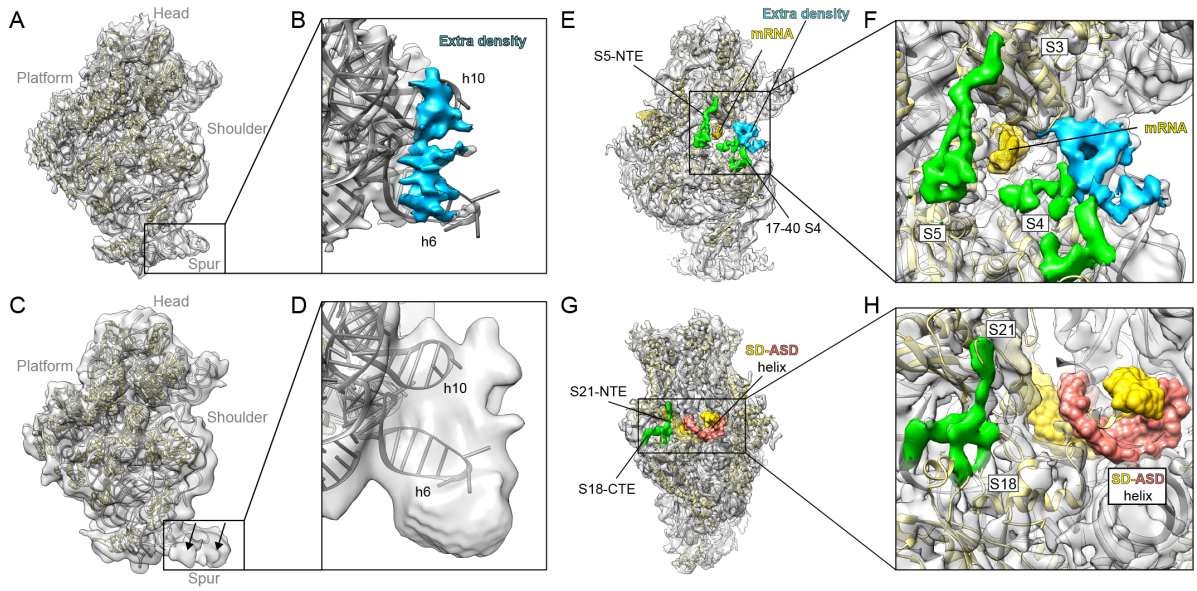

Figure S3: Localization of extra density on the SSU. (**A**) Overview of the back of the cryo-EM map (grey) of the chloroplast SSU with molecular model (rRNA, grey; RPs, yellow), and with (**B**) zoom onto the spur region, showing extra density (blue). (**C**) Overview of the back of the cryo-EM map (grey) of the chloroplast SSU from Sharma and coworkers (4) with molecular model (rRNA, grey; RPs, yellow), and with (**D**) zoom onto the spur region, showing additional density that was assigned to PSRP2/3. (**E**) Overview and (**F**) zoom onto the back of the cryo-EM map (grey) of the chloroplast SSU with molecular model (rRNA, grey; RPs, yellow), with cpRP densities (green) and unassigned extra density (blue) shown relative to the position of mRNA (yellow; superimposed from PDB ID 3I8G (5)). (**G**) Overview and (**H**) zoom onto the platform of the cryo-EM map (grey) of the chloroplast SSU with molecular model (rRNA, grey; RPs, yellow) and cpRP densities (green) shown relative to the position of SD-aSD helix (yellow/red; superimposed from PDB ID 3I8G (5)).

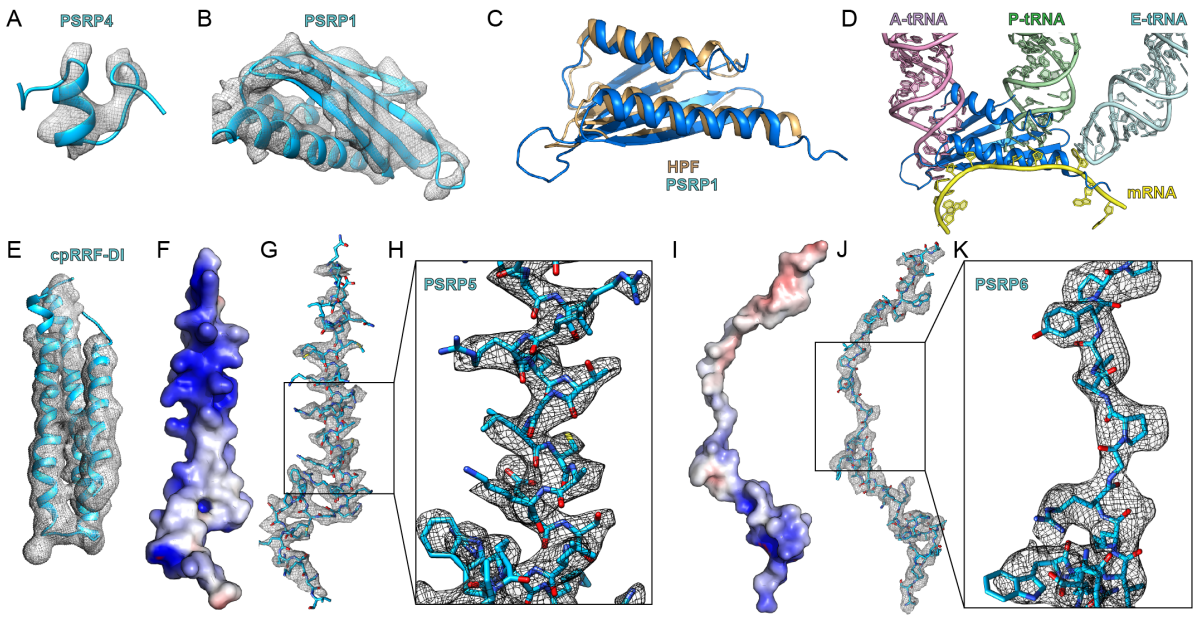

Figure S4: Localization of PSRPs on the chlororibosome. (**A,B**) Cryo-EM electron density (grey mesh) for (**A**) PSRP4 and (**B**) PSRP1. (**C,D**) Superimposition of the binding site of PSRP1 (blue) on the chlororibosome relative to (**C**) *E. coli* HPF (orange) bound to the *Thermus thermophilus* 70S ribosome (PDB ID 4V8H, (6)) and (**D**) mRNA (yellow) and A-site (pink), P-site (green) and E-site (cyan) tRNAs (PDB ID 3I8G, (5)). (**E**) Cryo-EM electron density (grey mesh) for domain I of the cpRRF (blue, cpRRF-DI). (**F-H**) Molecular model for PSRP5 shown as (**F**) surface charge (blue, positive) and (**G**) with electron density (grey mesh) and (**H**) zoom of the boxed region in (**G**). (**I-K**) Molecular model for PSRP6 shown as (**I**) surface charge (blue, positive, white neutral, red, negative) and (**J**) with electron density (grey mesh) and (**K**) zoom of the boxed region in (**J**).

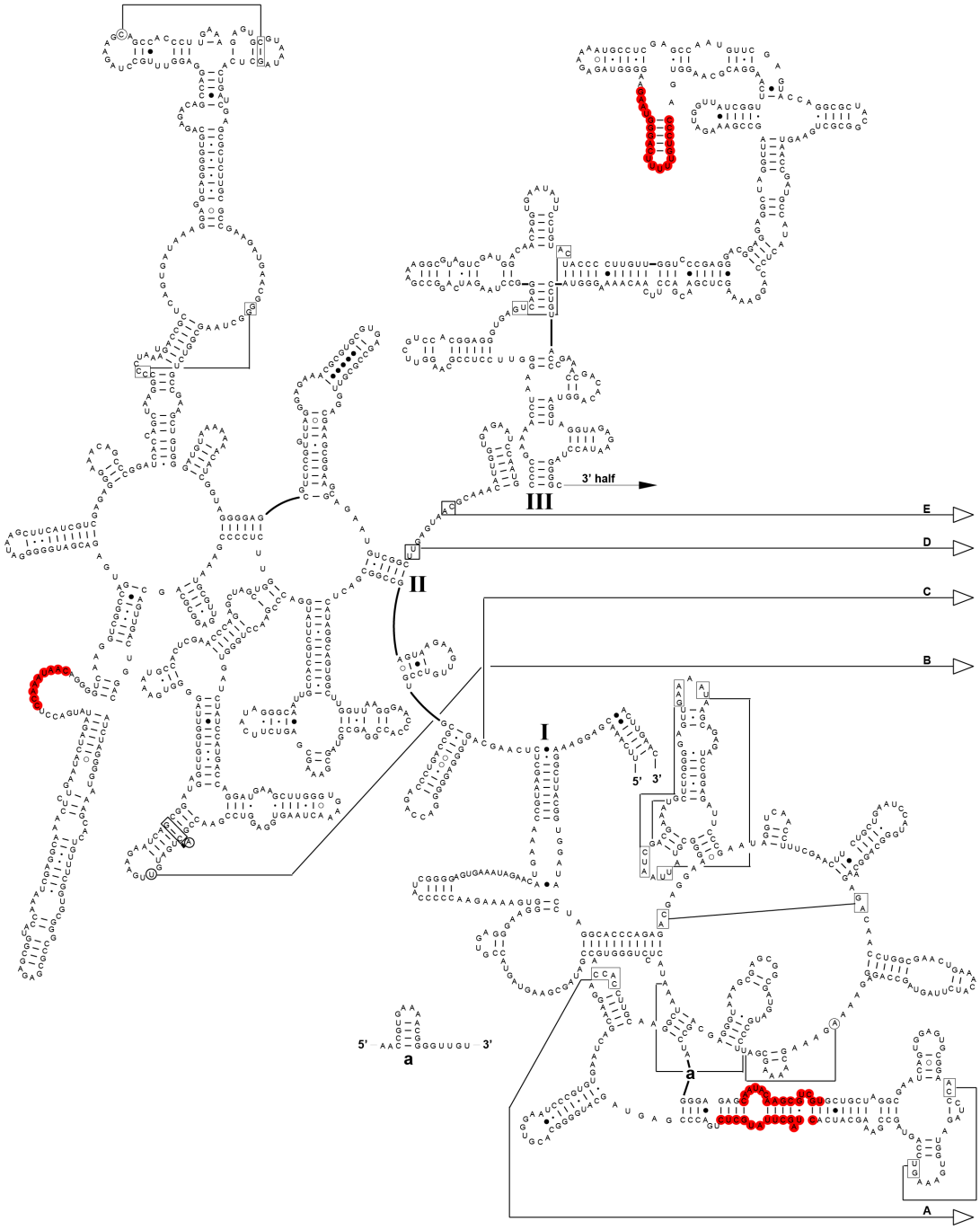

Figure S5: Modelled nucleotides of the chloroplast 4.8S and 23S rRNAs. (**A**) Secondary structure of the 5' portion of the cp23S rRNA, with nucleotides highlighted in red that were not modelled. The secondary structure diagram was taken from the Comparative RNA Web (CRW) Site (www.rna.ccbb.utexas.edu) (7).

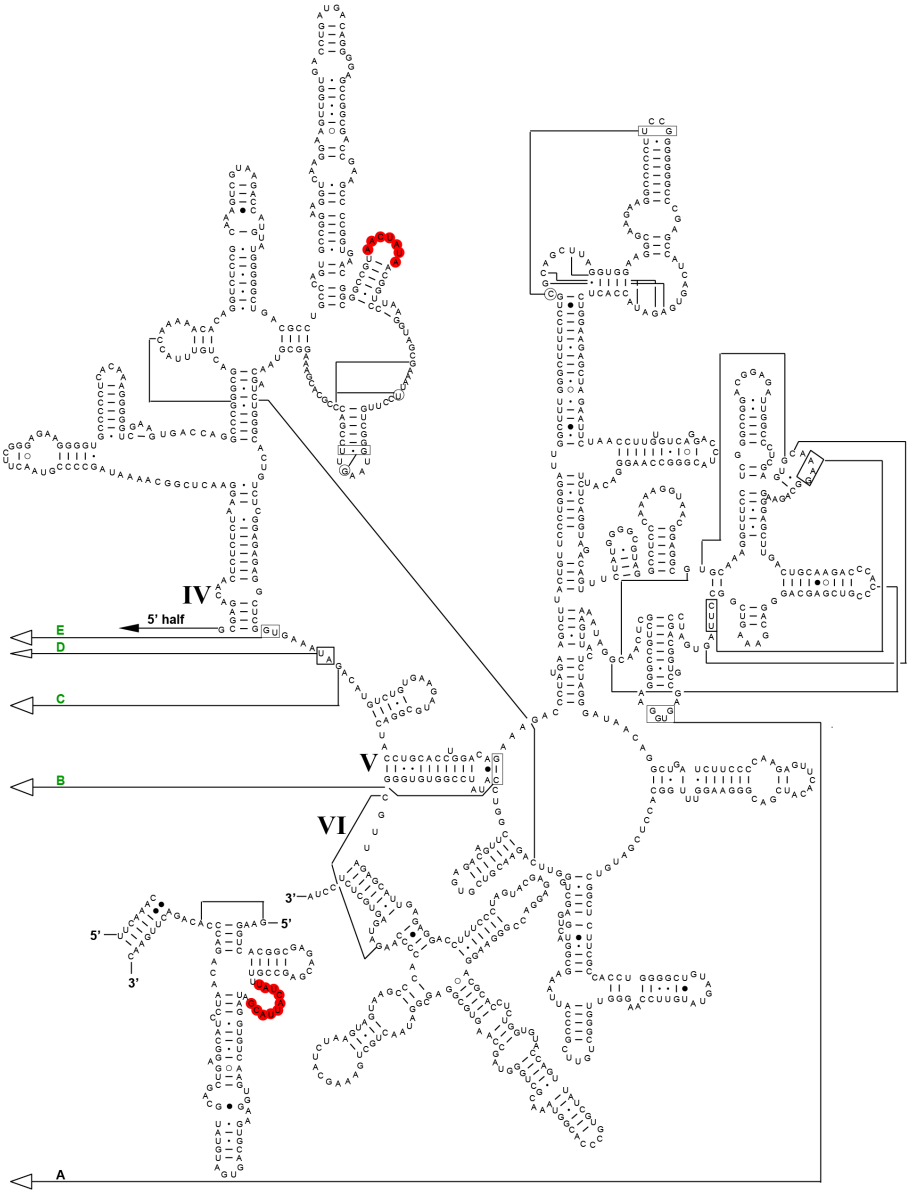

Figure S5: Modelled nucleotides of the chloroplast 4.8S and 23S rRNAs. (**B**) Secondary structure of the 3' portion of the cp23S rRNA and 4.8S rRNA, with nucleotides highlighted in red that were not modelled. The secondary structure diagram was taken from the Comparative RNA Web (CRW) Site (www.rna.ccbb.utexas.edu) (7).

SUPPLEMENTARY TABLES

Supplementary Table S1. Data collection and refinement statistics

Data Collection and Refinement	**Cp50S**
Particles	37,636
Pixel size (Å)	1.061
Defocus range (μm)	-1.0-2.3
Voltage (kV)	300
Electron dose ($e^-/Å^{-2}$)	40.3
Map sharpening B factor ($Å^2$)	-84.98
Resolution (Å, 0.143 FSC)	3.6
$FSC_{Average}$	0.88
Model Composition	
Protein residues	3,392
RNA bases	2,963
Validation (proteins)	
Poor rotamers (%)	7.11
Ramachandran outliers (%)	2.94
Ramachandran favored (%)	85.51
Bad backbone bonds (%)	0.04
Bad backbone angles	0.01
MolProbity score	2.48 (99^{th} percentile)
Validation (nucleic acids)	
Correct sugar puckers (%)	96.39
Good backbone conformations (%)	69.83
Bad bonds (%)	0.01
Bad angles	0.21
Clash score, all atoms	3.96 (100^{th} percentile)

Supplementary Table S2 Modeled proteins of the chloroplast LSU

Protein	UniProtKB	Preprotein	Mature Length	Modeled Residues
uL01c	Q9LE95	1-352	73-352	
uL02c	P06509		2-272	26-271
uL03c	A0A0K9QEC7	1-305	85-305	85-303
uL04c	O49937	1-293	51-293	56-260
uL05c	P82192		1-220	16-194
uL06c	A0A0K9R4N9	1-220	39-220	40-217
bL09c	A0A0K9RQ91	1-196	42-196	43-87
uL10c	A0A0K9R3N5	1-232	53-232	
uL11c	P31164	1-224	67-224	
bL12c	P02398	1-189	57-189	
uL13c	P12629	1-250	48-250	55-250
uL14c	P09596		1-121	1-120
uL15c	A0A0K9QHT0	1-271	61-271	78-259
uL16c	P17353		1-135	1-135
bL17c	A0A0K9RLJ4	1-126	11-126	11-126
uL18c	A0A0K9QQ60	1-166	45-166	49-166
bL19c	P82413	1-233	78-233	117-230
bL20c	P28803		2-128	2-117
bL21c	P24613	1-256	56-256	101-234
uL22c	P09594		2-199	25-176
uL23c	Q9LWB5	1-198	77-198	104-194
uL24c	P27683	1-191	47-191	47-175
bL27c	A0A0K9R4I2	1-194	57-194	59-166
bL28c	A0A0K9RD02	1-148	72-148	72-146
uL29c	A0A0K9R7W8	1-168	59-168	59-152
bL31c	A0A0K9R0R6	1-130	37-130	
bL32c	P28804	1-57	2-57	2-43
bL33c	P28805		1-66	6-65
bL34c	P82244	1-152	92-152	92-152
bL35c	P23326	1-159	87-159	90-159
bL36c	P12230		1-37	1-37
PSRP5	P27684	1-142	59-142	97-142
PSRP6	P82411	1-116	48-116	48-94
RRF	P82231		1-271	89-114;191-271

SUPPLEMENTARY REFERENCES

1. Kucukelbir, A., Sigworth, F.J. and Tagare, H.D. (2014) Quantifying the local resolution of cryo-EM density maps. *Nat. Methods*, **11**, 63-65.
2. Frank, J., Radermacher, M., Penczek, P., Zhu, J., Li, Y., Ladjadj, M. and Leith, A. (1996) SPIDER and WEB: processing and visualization of images in 3D electron microscopy and related fields. *J. Struct. Biol.*, **116**, 190-199.
3. Grigorieff, N. (2007) FREALIGN: high-resolution refinement of single particle structures. *J. Struct. Biol.*, **157**, 117-125.
4. Sharma, M.R., Wilson, D.N., Datta, P.P., Barat, C., Schluenzen, F., Fucini, P. and Agrawal, R.K. (2007) Cryo-EM study of the spinach chloroplast ribosome reveals the structural and functional roles of plastid-specific ribosomal proteins. *Proc. Natl. Acad. Sci. USA*, **104**, 19315-19320.
5. Jenner, L.B., Demeshkina, N., Yusupova, G. and Yusupov, M. (2010) Structural aspects of messenger RNA reading frame maintenance by the ribosome. *Nat. Struct. Mol. Biol.*, **17**, 555-560.
6. Polikanov, Y.S., Blaha, G.M. and Steitz, T.A. (2012) How hibernation factors RMF, HPF, and YfiA turn off protein synthesis. *Science*, **336**, 915-918.
7. Cannone, J.J., Subramanian, S., Schnare, M.N., Collett, J.R., D'Souza, L.M., Du, Y., Feng, B., Lin, N., Madabusi, L.V., Muller, K.M. *et al.* (2002) The comparative RNA web (CRW) site: an online database of comparative sequence and structure information for ribosomal, intron, and other RNAs. *BioMed Central Bioinformatics*, **3**, 2.